Alcaligenes xylosoxidans Dissimilatory Nitrite Reductase: Alanine Substitution of the Surface-Exposed Histidine 139 Ligand of the Type 1 Copper Center Prevents Electron Transfer to the Catalytic Center†

Miguel Prudêncio,‡,§ Gary Sawers,‡ Shirley A. Fairhurst,|| Faridoon K. Yousafzai,|| and Robert R. Eady*,||

Departments of Biological Chemistry and Molecular Microbiology, John Innes Centre, Norwich NR4 7UH, U.K.

Received October 22, 2001; Revised Manuscript Received January 14, 2002

ABSTRACT: Nitrite reductase of *Alcaligenes xylosoxidans* contains three blue type 1 copper centers with a function in electron transfer and three catalytic type 2 copper centers. The mutation H139A, in which the solvent-exposed histidine ligand of the type 1 copper ion was changed to alanine, resulted in the formation of a colorless protein containing 4.4 Cu atoms per trimer. The enzyme was inactive with reduced azurin as the electron donor, and in contrast to the wild-type enzyme, no EPR features assignable to type 1 copper centers were observed. Instead, the EPR spectrum of the H139A enzyme, with parameters of $g_1 = 2.347$ and $A_1 = 10$ mT, was typical of type 2 copper centers. On the addition of nitrite, the EPR features developed spectral features with increased rhombicity, with $g_1 = 2.29$ and $A_1 = 11$ mT, arising from the type 2 catalytic site. As assessed by visible spectroscopy, ferricyanide ($E° = +430$ mV) was unable to oxidize the H139A enzyme, and this required a 30-fold excess of K_2IrCl_6 ($E° = +867$ mV). Oxidation resulted in the EPR spectrum developing additional axial features with $g_1 = 2.20$ and $A_1 = 9.5$ mT, typical of type 1 copper centers. The oxidized enzyme after separation from the excess of K_2IrCl_6 by gel filtration was a blue-green color with absorbance maxima at 618 and 420 nm. The instability of the protein prevented the precise determination of the midpoint potential, but these properties indicate that it is in the range 700−800 mV, an increase of at least ~470 mV compared with the native enzyme. This high potential, which is consistent with a trigonal planar geometry of the Cu ion, effectively prevents azurin-mediated electron transfer from the type 1 center to the catalytic type 2 Cu site. However, with dithionite as reductant, 20% of the activity of the wild-type enzyme was observed, indicating that the direct reduction of the catalytic site by dithionite can occur. When $CuSO_4$ was added to the crude extract before isolation of the enzyme, the Cu content of the purified H139A enzyme increased to 5.7 Cu atoms per trimer. The enzyme remained colorless, and the activity with dithionite as a donor was not significantly increased. The additional copper in such preparations was associated with an axial type 2 Cu EPR signal with $g_1 = 2.226$ and $A_1 = 18$ mT, and which were not changed by the addition of nitrite, consistent with the activity data.

The process of denitrification, in which nitrate undergoes stepwise reduction to the gaseous products nitrous oxide and dinitrogen, forms one of the main branches of the global nitrogen cycle. In addition to its importance in microbial bioenergetics, further impetus for studying denitrification is provided by its environmental impact in generating N_2O as a potent greenhouse gas and as a process which removes polluting nitrate from groundwater (*1*−*3*). The conversion of nitrite to nitric oxide, catalyzed by dissimilatory nitrite reductases, is a key step in denitrification since it is the point at which fixed nitrogen in the soil is converted to a gaseous product, which can result in significant losses of nitrogen to the atmosphere.

Two classes of periplasmic nitrite reductases (NiR)[1] have been isolated from denitrifying microorganisms. One class of enzymes has cd_1 heme as the prosthetic group, while the second class includes enzymes that contain only copper. The copper-based NiRs are divided into two subclasses based on their color, being either blue or green (*3*). Crystallographic structures of two green NiRs, the enzymes from *Achromobacter cycloclastes* (AcNiR) (*4*−*6*) and *Alcaligenes faecalis* (AfNiR) (*7*), and the blue NiR from *Alcaligenes xylosoxidans* (AxNiR) (*8*−*10*) have been reported. These studies revealed that although these enzymes are trimers with very similar overall structures, they exhibit striking differences in surface

† This work was supported by the Biotechnology and Biological Sciences Research Council as part of the competitive strategic grant to the John Innes Centre and by a PRAXIS XXl studentship (BD 5451/95) to M.P.

* To whom correspondence should be addressed. Tel: +44 1603 450728. Fax: +44 1603 450018. E-mail: robert.eady@bbsrc.ac.uk.

‡ Department of Molecular Microbiology, John Innes Centre.

§ Present address: Leiden Institute of Chemistry, Gorlaeus Laboratories, Leiden University, 2300 RA Leiden, The Netherlands.

|| Department of Biological Chemistry, John Innes Centre.

[1] Abbreviations: NiR, nitrite reductase; AxNiR, nitrite reductase from *Alcaligenes xylosoxidans*; AcNiR, nitrite reductase from *Achromobacter cycloclastes*; AfNiR, nitrite reductase from *Alcaligenes faecalis*; RsNiR, nitrite reductase from *Rhodopseudomonas sphaeroides*; EPR, electron paramagnetic resonance; ENDOR, electron nuclear double resonance; EXAFS, extended X-ray absorption fine structure; MV, methyl viologen.

10.1021/bi011955c CCC: $22.00
Published on Web 02/12/2002

charge distribution (*9*). Each monomer contains two types of copper center: a type 1 center located in each subunit and a type 2 center located at the interface of adjacent subunits. The type 1 Cu ion is ligated by two His residues, one Met residue, and one Cys residue and exhibits strong bands at 450 and 600 nm arising from a (Cys)S−Cu(II) charge-transfer transition. The relative intensity of these bands in NiRs from different organisms determines the color as blue or green (*2*, *3*). A comparison of the structures of blue and green NiRs showed that the Cu−ligand distances were very similar and that the most significant structural difference between the type 1 sites was the His_c−Cu−Met angle (9). This, rather than the suggested differences in the length of the Cu−Met bond (*5*), may account for the colors of the enzymes from different organisms. The type 2 Cu ion is ligated by three His residues and a water molecule or OH^- ion, which in some preparations of AxNiR is replaced by a Cl^- ion.

The binding of NO_2^- to oxidized NiRs has been studied by a number of methods, and the findings indicate that a substantial rearrangement of the type 2 site occurs. X-ray crystallographic studies of AcNiR (*5*) and AxNiR (*8*, *9*) have shown that a bound water or an OH^- at the type 2 Cu ion is replaced by NO_2^-, which binds asymmetrically through both oxygen atoms. Studies of NO_2^- binding to AxNiR (*11*) and *Rhodopseudomonas sphaeroides* NiR (RsNiR) (*12*) showed perturbation of both ^1H and ^{14}N features of the ENDOR spectra of the type 2 center. In addition, difference Cu EXAFS studies of AxNiR have shown that on binding NO_2^- the average His−Cu distances of the type 2 Cu site increase by 0.08 Å, which may promote electron transfer from the type 1 Cu ion (*13*).

The consensus view of the mechanism of Cu-containing nitrite reductases when catalyzing the reaction:

$$NO_2^- + e^- + 2H^+ \rightarrow NO + H_2O$$

is that the type 1 Cu center functions in electron uptake from a reduced cupredoxin (an azurin in the case of *A. xylosoxidans*) (*14*) and electron transfer to the type 2 Cu site where NO_2^- binding and reduction occur. Pulse radiolysis studies of Cu-containing NiRs have shown these two types of Cu center to be in redox equilibrium in the absence of substrate. The rapid reduction of the type 1 Cu(II) by radicals produced by pulse radiolysis is followed by a reversible electron-transfer reaction between the two Cu centers, which, in the case of AxNiR, has reported rate constants $k_{ET} = k_{1,2} + k_{2,1}$ ranging from 1400 s^{-1} (*15*, *16*) to 450 s^{-1} (*17*). Comparative EXAFS, EPR, and UV−vis spectroscopies and activity studies of oxidized and reduced AxNiR (*18*) have shown that the reduced type 2 Cu center no longer binds the inhibitor azide, and the reduced NiR is inactive with ascorbate/PMS as reductant. On the basis of these findings, an ordered mechanism has been proposed for AxNiR (*18*) in which nitrite binds to an oxidized type 2 center to trigger electron transfer from a reduced type 1 center.

Previous mutational studies of type 1 centers of green NiRs have focused on the methionine ligand to the Cu, which has been mutated to threonine in RsNiR (*19*) and glutamate in AfNiR (*20*). The structure of the mutated AfNiR showed no significant differences from the native structure other than a local perturbation of the type 1 center with the glutamate residue bound via one oxygen atom to the metal, which anomalous scattering data showed to be zinc (*21*). The effect of this substitution was to prevent activity with reduced pseudoazurin as the electron donor, but activity with reduced MV was largely retained (*20*). In the case of RsNiR, the type 1 center became blue, rather than blue-green, and a 100 mV increase in the E_m of this center occurred. Despite this increase in potential, activity with reduced cytochrome *c* as an electron donor was retained, albeit at a lower level than with the wild-type enzyme (*19*). These authors proposed that the E_m of the type 2 center was increased so as to promote electron transfer from the type 1 site.

We report here the first mutational studies for the type 1 Cu center of a blue NiR. The aim of the present study was to generate mutations in the ligands to the type 1 Cu center of AxNiR, which perturb the redox potential sufficiently to prevent electron transfer from this site to the type 2 Cu catalytic site. Mutation of the surface-exposed Cu ligand His139 to a nonligating Ala residue resulted in an enzyme with a catalytically competent type 2 Cu center for nitrite binding and reduction but one with a type 1 center unable to transfer electrons to the catalytic type 2 center.

EXPERIMENTAL PROCEDURES

Bacterial Strains, Plasmids, and Growth Media. The *Escherichia coli* strains used in this study were JM109 F′ *tra*D36 *lac*I^q Δ(*lac*Z)M15 *pro*A^+B^+/e14$^-$(McrA$^-$) Δ(*lac-pro*AB) thi *gyr*A96(Nal^r) *endA1 hsdR17* ($r_K^-m_K^+$) *rel*A1 *sup*E44 *rec*A1 (*22*), BL21(DE3) F^- *omp*T *gal [dcm] [lon] hsd*S_B ($r_B^-m_B^-$; an *E. coli* B strain) with DE3, a λ prophage carrying the T7 RNA polymerase gene (*23*), and Epicurian coli XL1-Blue (Stratagene). The plasmids used were pUC19 (Ap^R) (*22*), pBR322 (Ap^R) (*24*), pET28a (Kan^R) (Novagen), and pEnirsp-1, which is similar to pET28a but includes the *A. xylosoxidans nirA* gene under the control of the phage T7 ϕ10 gene promoter (*25*). Antibiotics were used at a final concentration of 50 μg/mL.

Bacteria were grown routinely at 37 °C in Luria broth (LB), [1% w/v bactotryptone (Difco), 0.5% w/v yeast extract (Difco), 1% w/v NaCl]. Small-scale cultures (up to 10 mL) for plasmid DNA isolation were grown aerobically in conical flasks filled to approximately 10% of their volume with growth medium. Large-scale growths (200 L) used for isolation of NiR were cultured in New Brunswick fermentors under the control of Bio-Command software, with a dissolved oxygen concentration of 20% air saturation. Media were supplemented with $CuSO_4$ (1 mM) and the appropriate antibiotic solution. Antibiotics were purchased from Sigma, and stock solutions were prepared in water and filter-sterilized through sterile 0.2 μm syringe filters (Sartorius). Induction of high-level protein production was initiated when the cultures had reached the late exponential phase of growth, through the addition of 0.5 mM isopropyl β-D-thiogalacto-pyranoside (IPTG). Growth was continued for a further 90 min after which time the cells were harvested by centrifugation. Cells were used immediately for the isolation of NiR or were stored frozen at − 80 °C until required.

Site-Directed Mutagenesis. Site-directed mutagenesis of the *nirA* gene in plasmid vector pEnirsp-1 (*25*) was performed with the QuikChange site-directed mutagenesis kit (Stratagene), following the instructions of the manufacturer.

The oligonucleotides used to construct the *nirA* gene mutant were H139A-F (5′-GGTGCCCTGGGCCGTGGTGTCGGG-3′) and H139A-R (5′-CCCGACACCACGGCCCAGGGCA-CC-3′). The resulting plasmid was termed pEnirH139A, which encoded the NiR mutant H139A. The complete DNA sequence of the mutant *nirA* gene was verified using the method of Sanger et al. (*26*).

Protein Purification. AxNiR was purified from the periplasmic fraction of recombinant *E. coli* cells using a single carboxymethylcellulose step as described previously (*25*). Wild-type AxNiR, either isolated from *A. xylosoxidans* (*27*) or overexpressed in *E. coli* (*25*), has a pronounced absorbance band at 595 nm characteristic of an oxidized type 1 Cu center allowing the blue color to be utilized to follow purification. In the present case, following elution of unbound proteins, the tight dark blue band at the top of the column characteristic of bound recombinant AxNiR was not observed. The column was developed with 20 mM Tris-HCl buffer, pH 7.0, containing 50 mM NaCl and the major peak monitored at 280 nm collected. In addition, some of the H139A mutant AxNiR was purified from the periplasmic extract previously dialyzed against 1 mM $CuSO_4$, a procedure necessary for full incorporation of Cu into the type 2 centers of both wild-type and recombinant NiRs (*25, 27*). Azurin 1 was isolated from *A. xylosoxidans* as described previously (*14*).

Oxidation of NiR H139A^{Cu}. In a typical experiment, AxNiR in 100 mM Tris-HCl buffer, pH 7.1, containing 5 mM NO_2^- was titrated with 10 μL aliquots of a solution of hexachloroiridate (20 mM, dissolved in water). After an equilibration period of 1−2 min the UV−vis spectrum was recorded. When no further change in absorbance was noted, the mixture was separated on a small desalting column of P6DG (Bio-Rad) equilibrated with 100 mM Tris-HCl buffer, pH 7.1, containing 5 mM $NaNO_3$.

Metal Determination. The copper and zinc contents of samples of NiR were measured on wet-ashed samples (*27*), using inductively coupled plasma emission spectroscopy by Southern Analytical (Brighton, Sussex, U.K.).

Spectroscopic Methods. EPR data were collected with a Bruker ER200 D-SRC spectrometer fitted with an ER042 MRH X-band microwave bridge and an Oxford Instruments ESR-900 liquid helium flow cryostat and ITC 503 temperature controller. Spectra were recorded at 60 K with a microwave power of 2 mW. EPR spectra were simulated using the program WINEPR-SimFonia (Bruker). Spin quantitation was made according to the method of Åasa and Vänngård (*28*) by comparing the area of the experimental curve under nonsaturating conditions to that obtained, under the same conditions, for a sample of Cu(II)-EDTA.

Nitrite Reductase Activity Assays. Nitrite reductase activity of recombinant and mutant forms of the enzyme was determined using methyl viologen (MV), sodium dithionite, or the physiological electron donor reduced azurin, as described (*29*). The stopped-time MV assay for nitrite reductase activity measures the amount of nitrite utilized during the assay period by determination of residual nitrite by diazotization (*27*). In such assays the time dependence or NiR concentration dependence was established. Under these conditions the nonenzymatic reaction of nitrite was less than 5% after a 30 min incubation period. In all assays involving dithionite the appropriate minus-enzyme controls were run and the small corrections to the enzymatic rates were made. In the continuous spectrophotometric assays the oxidation of dithionite or azurin was monitored directly, and the nitrite concentration was 1 mM. In all assays, one unit of enzyme activity is defined as the oxidation/reduction of 1 μmol of electron donor/nitrite per minute.

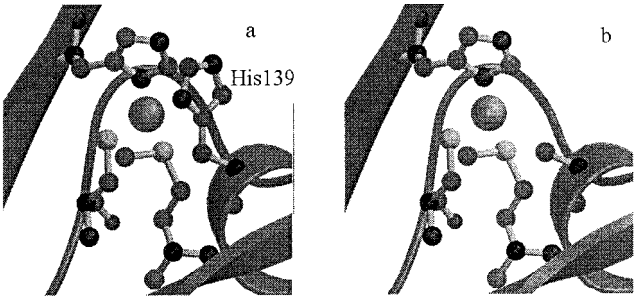

FIGURE 1: Amino acid residues and ligand geometry of the type 1 Cu site of (a) wild-type AxNiR and (b) simulation of the site in a mutant protein where His139 has been replaced by alanine (AxNiR H139A). In the wild type the $N^{\epsilon 2}$ atom of His139 is oriented such that it is exposed to the solvent.

Electrophoresis of Proteins. Polyacrylamide gel electrophoresis in the presence of sodium dodecyl sulfate (SDS−PAGE) was used routinely to monitor the purity of protein samples throughout the purification of NiR and to assess the levels of overproduced recombinant NiR proteins. SDS−PAGE was performed according to Laemmli (*30*). Typically, 12.5% (w/v) or 15% (w/v) acrylamide gels were run.

Determination of Protein Concentration. Protein determinations were carried out by the method of Lowry et al. (*31*). For pure preparations of NiR the protein concentration was estimated using an extinction coefficient at 280 nm (ϵ_{280}) of 1.54 $mg^{-1}\cdot mL^{-1}\cdot cm^{-1}$ (F. K. Yousafzai, unpublished).

RESULTS AND DISCUSSION

The crystal structures of AxNiR (*8*−*10*) have defined the location and geometry of the Cu sites of the enzyme. The two Cu atoms of the type 1 and type 2 centers are 12.6 Å apart and are directly connected by Cys130 and His129. The ligands to the type 1 copper ion are provided by the N-terminal domain of a single subunit, and three of them, Cys130, His139, and Met144, originate in a small loop (residues 139−144), an arrangement also found in azurins (*1*). The metal is ligated by three strong planar ligands, the S^{γ} of Cys130 and the N^{δ} atoms of two histidine residues (His89 and His139), with the S^{γ} of Met144 in an axial position (see Figure 1a).

The location and environment of His139 are very similar to those of the solvent-exposed His117 in azurins where it is proposed to have a role in electron transfer (*1*). It has been shown that the mutation of the analogous His117 of *Pseudomonas aeruginosa* azurin to Gly considerably enhances the flexibility of the loop containing three of the four ligands to the Cu in the wild-type protein (*32*). This mutant has an unusually high redox potential of 670 ± 10 mV (*33*) due to the reduced center adopting a stabilized 3-fold coordination (*34*). We constructed the H139A mutant form of AxNiR, in which the imidazole group of His139 is replaced by a smaller nonligating residue with an aliphatic hydrocarbon side chain, and investigated the effects of this mutation on the properties of AxNiR. By analogy with the H117G mutant of azurin the vacant position left in the type

Table 1: Copper Content of the Two Forms of the H139A Mutant of AxNiR[a]

	EPR-detectable Cu (atoms/trimer)	total Cu (atoms/trimer)
$H139A^{Cu}$	2.7 (signal A + signal B)	5.7
H139A	1.7 (signal A)	4.4

[a] The total Cu content was determined by ICP analysis and EPR-detectable Cu by comparison of double integration with a Cu-EDTA standard. The $H139A^{Cu}$ protein was purified from a periplasmic extract after supplementation with 1 mM $CuSO_4$. The H139A protein was purified from the same batch of cells, but no Cu was added to the periplasmic fraction.

1 Cu center of AxNiR by the mutation of His139 is likely to be H_2O or OH^-. The effect of the H139A mutation of AxNiR in potentially opening the site and exposing the Cu ion to solvent is shown in Figure 1b.

Construction and Purification of the H139A Mutant of AxNiR. An overproducing strain of *E. coli* carrying the H139A mutation of AxNiR was constructed and grown as described in Experimental Procedures. The mutant form of AxNiR was purified from periplasmic extracts of *E. coli* essentially as described for the recombinant wild-type enzyme (*29*). Copper analysis of the purified enzyme gave a Cu content of 4.4 Cu atoms per trimer, indicating that the six potential Cu-binding sites were not fully loaded (Table 1). A similar partial occupancy of the copper-binding sites is observed when wild-type AxNiR is purified from *A. xylosoxidans* (*27*) or the recombinant enzyme from *E. coli* (*29*), if Cu is not added to the crude extracts before isolation of the enzyme. When $CuSO_4$ (1 mM) was added to the periplasmic extract before purification, the Cu content of the purified H139A mutant enzyme (designated $H139A^{Cu}$) increased to 5.7 Cu atoms per trimer. EPR spectroscopy (see below) showed the Cu to be incorporated into the type 2 sites, which were otherwise only partially loaded with metal. However, in contrast to the wild-type enzyme, the specific activity of the mutant protein did not increase significantly following Cu insertion. In both species of AxNiR H139A the EPR-detectable Cu was less than the total Cu measured by plasma emission spectroscopy (Table 1). To gain insight into the differences between the mutant proteins with and without fully loaded metal centers, both forms of the H139A AxNiR were characterized further.

Optical and EPR Spectroscopy of the Copper Sites of H139A AxNiR as Isolated. Both wild-type AxNiR isolated from *A. xylosoxidans* and the recombinant form overexpressed in *E. coli* exhibit an absorbance maximum in the visible region around 600 nm, characteristic of oxidized type 1 copper centers (*2*, *25*). Unexpectedly, both the purified H139A and the $H139A^{Cu}$ forms of the NiR mutant were colorless, even at concentrations as high as 40 mg/mL. In addition, the EPR spectra of both forms did not exhibit axial features characteristic of the presence of type 1 Cu centers.

The spectrum of H139A (Figure 2a) appeared more rhombic with four well-resolved Cu hyperfine lines and some partially resolved N hyperfine features. Neglecting the contribution from nitrogen superhyperfine splitting, simulation of this spectrum (designated as signal A) gave a Cu hyperfine splitting value (A_1) consistent with the EPR signals arising from a type 2 center but different from those of native AxNiR, which typically are $g_1 = 2.355$ and $A_1 = 9.0$ mT

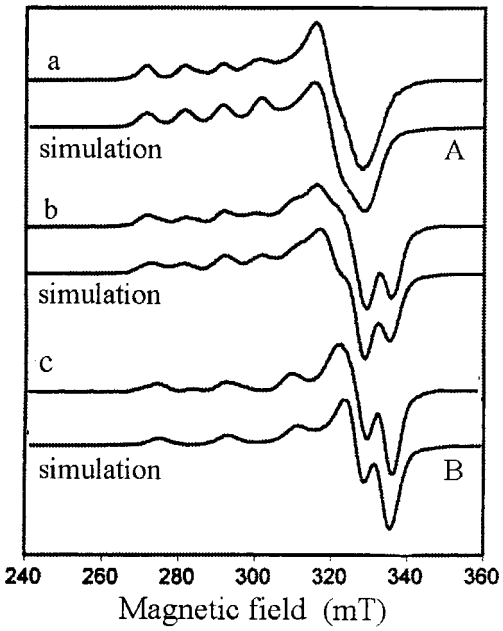

FIGURE 2: EPR spectra of AxNiR H139A and AxNiR $H139A^{Cu}$ as isolated. EPR spectra of (a) H139A (designated signal A) and (b) $H139A^{Cu}$ and (c) difference spectrum between (a) and (b) (designated signal B). The simulations of the spectra are shown beneath the experimental spectra. EPR spectra of H139A (43.6 mg/mL) and $H139A^{Cu}$ (22.1 mg/mL) in 100 mM Tris-HCl buffer, pH 7.1, were recorded at 60 K, 2 mW power, and a microwave frequency of 9.40 GHz. To facilitate comparison, spectra have been normalized to the same protein concentration. $H139A^{Cu}$ was purified from a periplasmic extract after supplementation with 1 mM $CuSO_4$, and H139A protein was purified from the same batch of cells but no Cu was added to the periplasmic fraction.

(*11*). This suggests that the geometry of the type 2 center is perturbed in the mutant as a consequence of the mutation of a type 1 ligand. Since the two Cu ions are 12.6 Å apart and connected by the adjacent ligands Cys130 and His129, mutation of a type 1 ligand, which resulted in an increase in mobility of the Cu ion, might be expected to be detected at the type 2 Cu site. Consistent with this, X-ray crystallographic studies of AxNiR with the type 1 center substitution M144A have shown that a small movement of the ligating histidine residues to the type 2 Cu ion occurs (S. Hasnain, personal communication). As shown below, the binding of nitrite to H139A changes the EPR signal to essentially restore the parameters to those of the wild-type AxNiR with nitrite bound. This suggests that the type 2 Cu site of the mutant and wild-type enzyme assumes a similar geometry when substrate is bound.

Surprisingly, a more complex type 2 EPR spectrum was obtained for the $H139A^{Cu}$ protein purified after incubation of the periplasmic fraction with $CuSO_4$. The spectrum shown in Figure 2b is clearly composed of two overlapping type 2 Cu signals. Subtraction of this spectrum from H139A resulted in the spectrum shown in Figure 2c, and simulation of this difference spectrum (hereafter designated signal B) gave a Cu hyperfine splitting value (A_1) consistent with the additional EPR associated with $H139A^{Cu}$ arising from a typical axial type 2 center with some unresolved features. These results (summarized in Table 2) show that the form of the type 2 Cu EPR signal in the H139A enzyme depends on whether the Cu atoms in this center are incorporated during the growth of the cells. The EPR signal of the type 2 Cu

Table 2: Summary of the EPR Parameters of the Different Type 2 Cu Centers of H139A and H139A^{Cu} Showing the Effect of Addition of Nitrite and Oxidation with K_2IrCl_6

NiR	EPR parameters						copper center
	g_1	A_1	g_2	A_2	g_3	A_3	
H139A	2.347	10.0	2.107	0	2.045	0	type 2, signal A
H139A^{Cu}	2.347	10.0	2.107	0	2.045	0	type 2, signal A
	2.226	18.0	2.056	0	2.056	0	type 2, signal B
H139A plus nitrite	2.290	11.0	2.085	3.0	2.016	6.8	itermediate type 1/type 2 signal C
H139A^{Cu} plus nitrite	2.290	11.0	2.085	3.0	2.016	6.8	itermediate type 1/type 2 signal C
	2.24	17.5	2.05	0	2.05	0	signal B*
H139A oxidized by K_2IrCl_6	2.347	10.0	2.107	0	2.045	0	type 2, signal A
	2.20	9.5	2.046	0	2.046	0	type 1

center incorporated in vivo exhibits only signal A, whereas the protein isolated from the periplasmic fraction incubated with $CuSO_4$ has an additional type 2 Cu species which exhibits signal B. A comparison of the integrated areas corresponding to each one of these two signals showed that they contribute 60% and 40%, respectively, to the spectrum of the H139A^{Cu} enzyme (Figure 2b). Since the type 2 Cu signal is dependent upon the environment of the Cu ion in this site and shows some variability for different preparations of NiR (*11*, *27*), these two signals appear to correspond to two different forms of the type 2 Cu center. As discussed below, only signal A is changed significantly by the addition of substrate. Crystallographic studies have shown that, depending on the protein preparation, AxNiR can have either water (*8*) or Cl^- (*9*) as the fourth ligand. Such differences may account for the variability in the EPR parameters we observe.

Properties of the Type 1 Cu Centers of H139A NiR. Previous studies of engineered mutations of His ligands to the type 1 Cu site in azurin have shown that these residues are not essential to maintain a type 1 Cu center (reviewed in refs *35* and *36*). Since the Cu content of H139A^{Cu} approached that expected for an enzyme with a full occupancy of the Cu-binding sites (Table 1), the absence of EPR signals assignable to a type 1 Cu center was surprising. The structural similarities of NiR with azurins would suggest that the H139A mutant of AxNiR was not type 1 Cu-depleted but that these centers were reduced in the protein as isolated and, therefore, spectroscopically silent when analyzed by the techniques used.

To test this possibility, attempts were made to oxidize the H139A protein with a 5-fold molar excess of potassium ferricyanide ($E^o = +430$ mV), relative to the estimated type 1 Cu content of the enzyme. However, the UV−vis spectrum of H139A remained unchanged even after 90 min incubation with this oxidant (data not shown), indicating that the potential of the putative type 1 Cu center in H139A must be higher than the potential of potassium ferricyanide. To oxidize the Cu in the type 1 centers, a stronger oxidant, potassium hexachloroiridate(IV) [K_2IrCl_6, $E^\circ = +867$ mV (*37*)], was used. A 5 mg/mL solution of H139A in 100 mM Tris-HCl, pH 7.1, was titrated with K_2IrCl_6, and UV−vis spectra were recorded after 2 min incubation. When the concentration of K_2IrCl_6 was ∼1 mM, approximately 7.5-fold molar excess over the estimated type 1 Cu content of the protein, an absorption band in the 600 nm region of the spectrum started to appear (Figure 3a) and the solution became greenish blue in color.

The absorption in this region continued to increase upon addition of up to ∼4.5 mM (∼30-fold molar excess) of oxidant and did not change further for concentrations of K_2IrCl_6 up to 6.5 mM (∼50-fold molar excess).

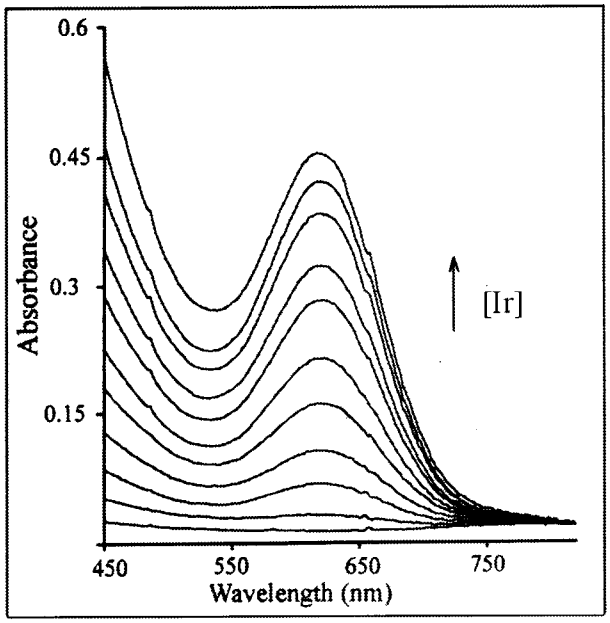

FIGURE 3: UV−vis spectra of AxNiR H139A^{Cu} during titration with the oxidant K_2IrCl_6. Spectra were recorded at room temperature after the addition of increasing amounts of K_2IrCl_6 to the enzyme in 5 mg/mL in Tris-HCl buffer, pH 7.5. Spectra were taken 1 min following addition of oxidant and have been normalized for the absorbance at 820 nm to correct for some precipitation that occurred at high oxidant concentrations.

Our attempts to measure the redox potential of the type 1 site by dye-mediated potentiometry were frustrated by the instability of the mutant protein leading to precipitation in the presence of high K_2IrCl_6 concentrations. However, using the data for ferricyanide and assuming that up to a 10% oxidation might have been undetected in the absorbance measurements, then the Nernst equation gives a minimum potential of the site of +708 mV. The requirement for a 30-fold excess of the more powerful oxidant K_2IrCl_6 suggests that the potential of the modified type 1 center lies in the range 700−860 mV, but the instability of AxNiR at high potentials precluded precise determination of the redox potential. Pulse radiolysis studies have shown that the Cu centers in wild-type AxNiR are in rapid redox equilibrium (*15*−*17*). Thus the presence of only the type 2 EPR signal in the mutant AxNIR as isolated indicates that one consequence of the mutation is to prevent electron transfer from the reduced type 1 Cu sites to the oxidized type 2 centers. We attribute this to the increase in E° of the type 1 Cu centers in the H139A enzyme.

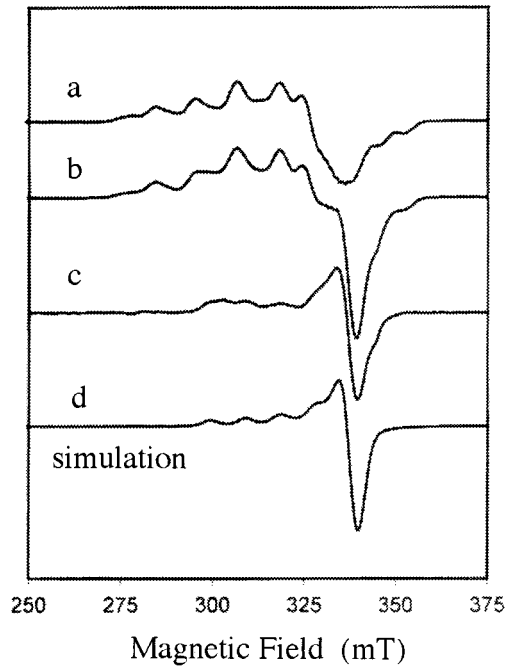

FIGURE 4: EPR spectra of K_2IrCl_6-oxidized AxNiR H139A: (a) H139A (43.6 mg/mL) in 100 mM Tris-HCl buffer, pH 7.1, and 5 mM NO_2^-, (b) oxidized H139A (16 mg/mL) in 100 mM Tris-HCl buffer, pH 7.1, and 5 mM NO_2^-, (c) difference spectrum of (a) and (b) normalized to the same integrated intensity to allow for dilution, and (d) simulation of the difference spectrum. Conditions for running EPR were as in Figure 2.

During this work we found that the presence of nitrite (5 mM) conferred some improvement in the stability of H139ANiR to excess K_2IrCl_6, and the oxidized protein could be separated from the mixture by rapid gel filtration. The absorbance spectrum of the separated material had an absorbance maximum in the visible range at 618 nm, which corresponds to a shift of ~22 nm to higher wavelength with regard to native NiR. Below this wavelength the absorbance increases to a second partially resolved peak at 420 nm, a feature normally associated with naturally occurring green type 1 Cu sites of AcNiR and AfNiRs (*1*).

EPR Signals Associated with K_2IrCl_6-Oxidized Enzyme. The EPR spectrum of the K_2IrCl_6-oxidized enzyme in the presence of nitrite is shown in Figure 4a. Compared with the enzyme as isolated in the presence of nitrite (Figure 4b), additional features are present, as is apparent from the difference spectrum (Figure 4c). Simulation of this difference spectrum (Figure 4d) gave values of $g_1 = 2.20$ and $A_1 = 9.5$ mT. The positions of these values on a Vänngård−Peisach−Blumberg plot (*39*, *40*), in which g_1 and A_1 show an approximately linear correlation for a particular type of Cu site, are in the range reported for type 1 centers. However, consistent with changes in the visible absorbance spectrum discussed above, the EPR parameters indicate that this site is perturbed relative to the native enzyme, which has values of $g_1 = 2.208$ and $A_1 = 6.6$ mT (*27*). These spectroscopic data indicate that, in the enzyme as isolated, the type 1 Cu center is reduced and the type 2 Cu center is oxidized.

Nitrite Binding to H139A Monitored by EPR Spectroscopy. When nitrite binds to wild-type AxNiR, the EPR spectrum of the type 2 Cu center shows a decrease in g_1 and an increase in A_1 (*11*, *41*). We used this property to monitor nitrite binding to the type 2 Cu site in H139A. The H139A protein used in this experiment had an estimated type 2 Cu content of 1.7 atoms per trimer (Table 1) and was titrated with various amounts of $NaNO_2$ up to a final concentration of 45 mM, and the EPR spectra thus obtained were recorded. The EPR spectra corresponding to the stages in the transition from H139A without nitrite to H139A in the presence of excess nitrite are shown in Figure 5. The insert of Figure 5 shows an expansion of the low-field region of these spectra, demonstrating the changes in the g_1 and A_1 parameters. As occurs with native AxNiR, the g_1 value of the type 2 centers in H139A decreases with increasing concentrations of nitrite while A_1 increases. Simulation of the EPR spectrum of H139A in the presence of excess nitrite gave values of $g_1 = 2.290$ and $A_1 = 11.0$ mT (hereafter called signal C; see below), as opposed to the initial values of $g_1 = 2.35$ and $A_1 = 10.0$ mT. In contrast to the spectrum of wild-type AxNiR, which shows axial symmetry, both signals A and C show considerable rhombicity. The change in ligand geometry of the type 2 centers associated with the binding of nitrite to AxNiR detected by EXAFS spectroscopy (*13*) may be responsible for the increased rhombicity shown by spectrum C. Consistent with this, ENDOR spectroscopy of AxNiR (*11*) and RsNiR (*12*) shows extensive perturbation of both ^1H and ^{14}N features of the type 2 spectrum in the presence of nitrite.

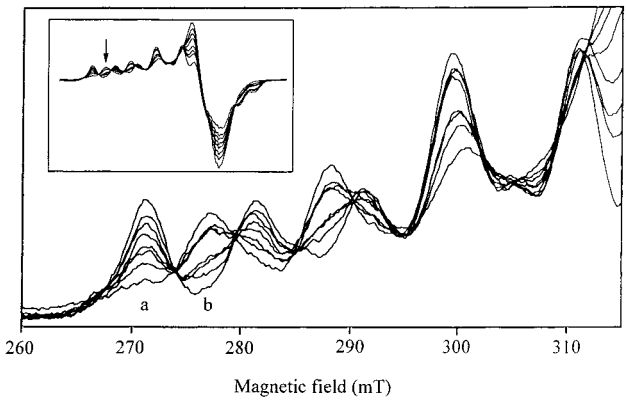

FIGURE 5: EPR spectra of AxNiR H139A during titration with NO_2^-. Various volumes of NO_2^- solution up to a final concentration of 45 mM were added to AxNiR H139A in 100 mM Tris-HCl buffer, pH 7.6. Spectra were normalized to the same integrated intensity to allow for dilution. (a) AxNiR H139A alone (signal A); (b) AxNiR H139A in the presence of excess NO_2^- (signal C). Main figure: an expansion of the low-field region of the spectrum demonstrating that only two species contribute to the type 2 Cu EPR spectra during the transition from free to the NO_2^--bound form is shown. The arrow in the insert indicates where the measurements to determine the binding constant for nitrite were taken. Conditions for running EPR were as in Figure 2.

The presence of the isoclinic points in the spectra shows that only two species are involved in this process, thus allowing the corresponding changes to be quantified. The intensity of the EPR spectra was plotted against the ratio of nitrite and type 2 Cu molar ratios, and the data were fitted assuming an equilibrium between the bound and unbound species. The analysis of the binding curves for the NO_2^--induced change in type 2 Cu EPR gave a best-fit binding constant for H139A at pH 7.1 of ~1 mM, approximately 3-fold higher than that determined for nitrite binding to NiR at pH 7.5 (*41*). The similarity between these two binding constants for species of AxNiR with the type 1 Cu ion reduced and oxidized, respectively, indicates that the oxida-

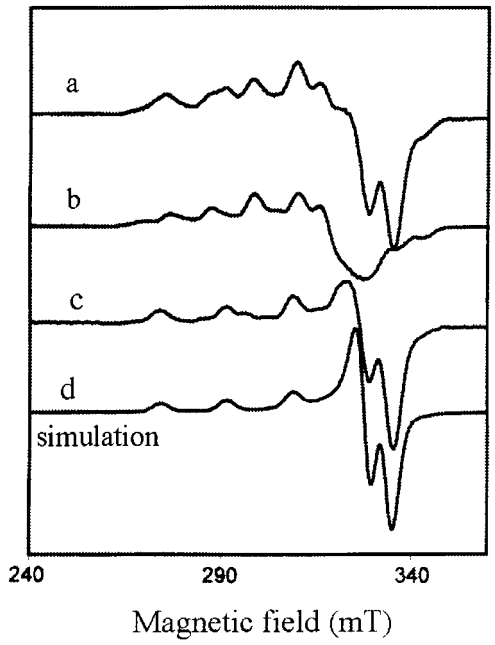

FIGURE 6: EPR spectra of AxNiR H139A and AxNiR H139A^{Cu} in the presence of excess NO_2^-: (a) H139A (43 mg/mL); (b) H139A^{Cu} (22 mg/mL) in the presence of a 20-fold excess over the type 2 Cu site concentration; (c) difference spectrum between (a) and (b); (d) simulation of the difference spectrum. Conditions for running EPR were as in Figure 2. Spectra have been normalized to the same protein concentration to facilitate comparison.

tion state of the type 1 Cu ion does not significantly change the affinity of the catalytic site for nitrite.

The EPR data in Figure 5 show that the form of the type 2 Cu site which generates the EPR signal A (Figure 2a), corresponding to the Cu incorporated during the growth of the cells, is functional in binding NO_2^- and is thus potentially catalytically competent. The question arises as to whether the form of the type 2 Cu center that generates signal B (Figure 2c), corresponding to the Cu incorporated upon reconstitution of the periplasmic fraction with $CuSO_4$, is capable of binding nitrite. To address this question, the H139A^{Cu} sample containing both forms of the type 2 Cu center was incubated with a 20-fold excess of nitrite. The resulting EPR spectrum (Figure 6a) was compared with that of the H139A sample containing only one form of the type 2 Cu center, also in the presence of excess nitrite (Figure 6b). When the EPR signal of sample H139A was subtracted from the EPR signal of sample H139A^{Cu}, the difference spectrum (Figure 6c) is dominated by a type 2 Cu signal with $g_1 = 2.32$ and $A_1 = 17.8$ mT, as determined from its simulation (Figure 6d). These parameters are very similar to the values of signal B, showing that this form of the type 2 Cu site, formed on the addition of Cu to crude extracts, does not bind nitrite. This is consistent with our finding that H139A^{Cu} and H139A have similar enzymatic activities (see below). This is in contrast with the native enzyme where the copper incorporated into the type 2 site in vitro is functional, and a center with normal EPR parameters is formed (*27*).

Enzyme Activity with Different Electron Donors. Mutation of the type 1 center is expected to result in changes in the ability of different electron donors to support enzymatic activity.

Table 3: Activity of the H139A Mutant of AxNiR with Different Electron Donors[a]

	electron donor		
	methyl viologen	dithionite	azurin
H139A^{Cu}	0.95 ± 0.1	20.5 ± 2	0
H139A	0.85 ± 0.1	16.4 ± 2	0

[a] The H139A^{Cu} protein was purified from a periplasmic extract after supplementation with 1 mM $CuSO_4$. The H139A protein was purified from the same batch of cells, but no Cu was added to the periplasmic fraction. The values are percent activity relative to recombinant wild-type enzyme; these values [μmol min^{-1} (mg of protein)$^{-1}$] were dithionite, 107; azurin, 84; and methyl viologen, 168.

The nitrite reductase activities of H139A and H139A^{Cu} were determined by three different methods and compared with those of wild-type recombinant NiR. We used two artificial electron donors, MV and dithionite, and a putative physiological electron donor, reduced azurin I (see Experimental Procedures for details). This approach potentially provides information on electron flow between type 1 Cu and type 2 Cu, as well as on accessibility to the Cu atoms in the catalytic site. The results obtained, summarized in Table 3, show little difference in the activity of the two forms of the H139A mutant protein, consistent with the EPR data which show that the additional Cu present in H139A^{Cu} does not bind nitrite.

However, there is a clear difference in the activity of both species, when compared with recombinant AxNiR, depending upon the nature of the electron donor. For both forms of the mutated enzyme, dithionite was the most effective electron donor, whereas MV functioned only very poorly, and no activity was observed with reduced azurin I as donor. These data indicate that electron transfer from the altered type 1 Cu center is prevented by the raised $E°$ and that the low activity supported with artificial donors is due to the direct reduction of the catalytic type 2 Cu site. The difference in activity with dithionite and MV as electron donors may arise from their different accessibility to the type 2 Cu site due to charge differences or the ability of $SO_2^{\bullet -}$ to act as an analogue of the substrate NO_2^- ion. The lack of activity with reduced azurin I, the physiological electron donor to the type 1 Cu center of NiR, is consistent with the type 1 centers of NiR being the route of entry for electrons derived from azurin. The consequence of the increase in the redox potential of the type 1 Cu site of AxNiR is effectively to prevent electron transfer from azurin via the type 1 Cu to the type 2 Cu in the H139A mutant.

CONCLUSIONS

The H139A mutation of the type 1 Cu centers of AxNiR results in a nitrite reductase that contains 4.4 Cu atoms per trimer but exhibits only a type 2 EPR spectrum. The mutation results in an unprecedented increase in the reduction potential of the type 1 Cu site, from +240 mV in the native enzyme to a value in the range 700−800 mV, an increase of at least ~470 mV. Naturally occurring type 1 Cu centers have a range of reduction potentials in different proteins ranging from +220 mV in *Ps. aeruginosa* azurin to +785 mV in *Polyporus vernicifera* laccase (see ref *36*). The role of the axial ligation in tuning reduction potentials of type 1 Cu sites has been established by a combination of mutagenesis and

X-ray structural studies. Additionally, the importance of the protein fold in generating sites with different hydrophobicity and solvent accessibility in modulating redox properties has been emphasized recently (see ref *36*). In the case of the H117G azurin mutation, reduction of the center results in the expulsion of the bound water ligand, and EXAFS studies show the Cu(I) ion to adopt a 3-fold coordination with a shortened Cu−S^{δ} (Met121) bond (*34*). Once reduced, re-oxidation of the center did not occur in the presence of excess $K_3Fe(CN)_6$ (*32*), as we observe for the H139A mutation of AxNiR. Given the strong structural homology of this site in AxNiR with azurins, this mutation is expected to create flexibility in the site to significantly stabilize the Cu(I) species, since a 3-fold coordination of the Cu atom favors the Cu(I) over the Cu(II) state (reviewed in ref *35*). It is noteworthy that the structures of both blue (*8*−*10*) and green (*4*−*7*) NiRs show that the type 1 centers have short Cu−S(Met) bond lengths in the oxidized and reduced (*13*) states, a factor which may contribute to the stabilization of the center in the H139A protein.

The electrochemical properties of the azurin mutant have recently been investigated by mediated potentiometric titration and shown to have a remarkably high reduction (midpoint) potential ($E^{o\prime}$) of +670 mV, an increase of 345 mV compared to the wild-type protein (*33*). These studies, together with our observations for AxNiR, emphasize the important role of the surface-exposed copper-coordinating histidine in modulating the redox activity of the type 1 Cu ion, both in a simple cupredoxin and also in AxNiR, a multi-copper-containing enzyme. This increase in the potential of the type 1 site of AxNiR effectively prevents electron transfer from the type 1 center to the catalytic site and renders the enzyme inactive with reduced azurin as an electron donor.

The EPR parameters and change in the spectrum from rhombic to axial symmetry indicate that the type 2 Cu center is perturbed by the mutation of the type 1 center but retains the ability to bind nitrite. The activity we observe with dithionite as an electron donor can be explained by the direct reduction of the type 2 Cu site. Unlike the native recombinant enzyme, the H139A mutation of AxNiR prevents the additional Cu, incorporated in the type 2 site by incubation of the enzyme with Cu in vitro, from binding nitrite. Hence, the increased Cu content does not result in an increase in specific activity. Crystallographic studies are in progress to determine the structural basis for this change in potential.

ACKNOWLEDGMENT

We thank Prof. Samar Hasnain, Dr. John Hall, and Mr. Llalji Kanbi for useful discussions. We are also grateful to Prof. Dr. Gerard Canters for communicating data on the properties of the mutant H117G azurin prior to publication.

REFERENCES

1. Zumft, W. G. (1997) *Microbiol. Mol. Biol. Rev. 61*, 533−616.
2. Averill, B. A. (1996) *Chem. Rev. 96*, 2951−2964.
3. Berks, B. C., Ferguson, S. J., Moir, J. W. B., and Richardson, D. J. (1995) *Biochim. Biophys. Acta 1232*, 97−173.
4. Godden, J. W., Turley, S., Teller, D. C., Adman, E. T., Liu, M. Y., Payne, W. J., and LeGall, J. (1991) *Science 253*, 438−442.
5. Adman, E. T., Godden, J. W., and Turley, S. (1995) *J. Biol. Chem. 270*, 27458−27474.
6. Kukimoto, M., Nishiyama, M., Murphy, M. E. P., Turley, S., Adman, E. T., Horinuchi, S., and Beppu, T. (1994) *Biochemistry 33*, 5246−5252.
7. Murphy, M. E. P., Turley, S., and Adman, E. T. (1997) *J. Biol. Chem. 272*, 28455−28460.
8. Dodd, F. E., Hasnain, S. S., Abraham, Z. H. L., Eady, R. R., and Smith, B. E. (1997) *Acta Crystallogr. D53*, 406−418.
9. Dodd, F. E., Van Beeumen, J., Eady, R. R., and Hasnain, S. S. (1998) *J. Mol. Biol. 282*, 369−38210.
10. Inoue, T., Gotowda, M., Deligeer, Kataoka, K., Yamaguchi, K., Suzuki, S., Watanabe, H., Gohow, M., and Kai, Y. (1998) *J. Biochem. 124*, 876−879.
11. Howes, B. D., Abraham, Z. H. L., Lowe, D. J., Brüser, T., Eady, R. R., and Smith, B. E. (1994) *Biochemistry 33*, 3171−3177.
12. Veselov, A., Olesen, K., Sienkiewicz, A., Shapleigh, J. P., and Scholes, C. P. (1998) *Biochemistry 37*, 6095−6105.
13. Strange, R. W., Dodd, F. E., Abraham, Z. H. L., Grössmann, J. G., Brüser, T., Eady, R. R., Smith, B. E., and Hasnain, S. S. (1995) *Nat. Struct. Biol. 2*, 287−292.
14. Dodd, F. E., Hasnain, S. S., Hunter, W. N., Abraham, Z. H. L., Debenham, M., Kanzler, H., Eldridge, M., Eady, R. R., Ambler, R. P., and Smith, B. E. (1995) *Biochemistry 34*, 10180−10186.
15. Suzuki, S., Kohzuma, T., Deligeer, Yamaguchi, K., Nakamura, N., Shidara, S., Kobayashi, K., and Tagawa, S. (1994) *J. Am. Chem. Soc. 116*, 11145−11146.
16. Suzuki, S., Deligeer, Yamaguchi, K., Kataoka, K., Kobayashi, K., Tagawa, S., Kohzuma, T., Shidara, S., and Iwasaki, H. (1997) *J. Biol. Inorg. Chem. 2*, 265−274.
17. Farver, O., Eady, R. R., Abraham, Z. H. L., and Pecht, I. (1998) *FEBS Lett. 436*, 239−242.
18. Strange, R. W., Murphy, L. M., Dodd, F. E., Abraham, Z. H. L., Eady, R. R., Smith, B. E., and Hasnain, S. S. (1999) *J. Mol. Biol. 287*, 1001−1009.
19. Oleson, K., Veselov, A., Zhao, Y. W., Wang, Y. S., Danner, B., Scholes, C. P., and Shapleigh, J. P. (1998) *Biochemistry 37*, 6086−6094.
20. Kukimoto, M., Nishiyama, M., Murphy, M. E. P., Turley, S., Adman, E. T., Horinuchi, S., and Beppu, T. (1994) *Biochemistry 33*, 5246−5252.
21. Murphy, M. E. P., Turley, S., Kukimoto, M., Nishiyama, M., Horinouchi, S., Sasaki, H., and Adman, E. T. (1995) *Biochemistry 34*, 12107−12117.
22. Yanish-Perron, C., Vieira, J., and Messing, J. (1985) *Gene 33*, 103−119.
23. Studier, F. W., and Moffat, B. A. (1986) *J. Mol. Biol. 189*, 113−130.
24. Bolivar, F., Rodriguez, R. L., Greene, P. J., Betlach, M. C., Heyneker, H. L., Boyer, H. W., Crosa, J. H., and Falkow, S. (1977) *Gene 2*, 96−113.
25. Prudêncio, M., Eady, R. R., and Sawers, G. (1999) *J. Bacteriol. 181*, 2323−2329.
26. Sanger, F., Nicklen, S., and Coulson, A. R. (1977) *Proc. Natl. Acad. Sci. U.S.A. 74*, 5463−5467.
27. Abraham, Z. H. L., Lowe, D. J., and Smith, B. E. (1993) *Biochem. J. 285*, 587−593.
28. Åasa, R., and Vänngård, T. (1975) *J. Magn. Reson. 19*, 308−315.
29. Prudêncio, M., Eady, R. R., and Sawers, G. (2000) *Biochem. J. 353*, 259−266.
30. Laemmli, U. K. (1970) *Nature 227*, 680−685.
31. Lowry, O. H., Rosebrough, N. J., Farr, A. L., and Randall, R. J. (1951) *J. Biol. Chem. 193*, 265−275.
32. Van Pouderoyen, G., Andrew, C. R., Loer, T. M., Sanders-Loer, J., Mazmdar, S., Hill, H. O. H., and Canters, G. W. (1996) *Biochemistry 35*, 1397−1407.
33. Jeuken, L. J. C., van Vliet, P., Verbeet, M., Camba, R., McEnvoy, J., Armstrong, F. A., and Canters, G. W. (2000) *J. Am. Chem. Soc 122*, 12186−12194.

34. Jeuken, L. J. C., Ubbink, M., Bitter, J. H., van Vliet, P., Meyer-Klaucke, W., and Canters, G. W. (2000) *J. Mol. Biol. 299*, 737−755.
35. Canters, G. W., and Gilardi, G. (1993) *FEBS Lett. 325*, 39−48.
36. Gray, H. B., Malmstrom, Bo. G., and Williams, R. J. P. (2000) *J. Biol. Inorg. Chem. 5*, 551−559.
37. Schilt, A. A. (1963) *Anal. Chem. 35*, 599−1602.
38. den Blaawen, T., and Canters, G. W. (1993) *J. Am. Chem. Soc. 115*, 1121−1129.
39. Vänngård, T. (1972) in *Biological Applications of Spin Resonance* (Swartz, H. M., Bolton, J. R., and Borg, D. C., Eds.) pp 411−417, Wiley-Interscience, New York.
40. Peisach, J., and Blumberg, W. E. (1974) *Arch. Biochem. Biophys. 165*, 691−708.
41. Abraham, Z. H. L., Smith, B. E., Howes, B. D., Lowe, D. J., and Eady, R. R. (1997) *Biochem. J. 324*, 511−516.

BI011955C